A Comparison of Two Methods of Measuring Particle Size of Al_2O_3 Produced by a Small Rocket Motor

R. A. DOBBINS*
Brown University, Providence, R. I.

AND

L. D. STRAND†
Jet Propulsion Laboratory, California Institute of Technology, Pasadena, Calif.

The size of the particulate effluent of rocket motors which contain aluminum as a fuel additive is required for the prediction of the thrust loss because of the particle lag, particulate radiant heat transfer, particulate acoustic attenuation, particle impingement, and plume structure and its properties. A further study of the particle size of the Al_2O_3 produced by a small rocket motor as determined by tank collection and by spectrophotometric tests was performed to rationalize a discrepancy and to learn to use these methods in a mutually complementary fashion. Tank collection tests were performed with tank volume, aluminum loading in the propellant, and chamber pressure as the principal variables. The particle size data from tank collection tests were analyzed in the form of various moment ratios and the mass median diameter. Spectrophotometric tests were performed at three wavelengths with motor chamber pressure and aluminum content as principal variables. The tank collection tests gave internally consistent results only when the mean size was defined in terms of the low moments of the distribution function. These mean diameters show the same mild growth with chamber pressure as indicated by the optical measurements. Evidence of particle growth resulting from velocity slip and collision in the nozzle was not found.

Nomenclature

a	= shape constant in size distribution function
c_v	= volume of particles per unit volume of gas
D	= diameter of particle
D_∞	= diameter of largest particle present in a given population or sample from a population
D_{PQ}	= generalized mean diameter as defined by Eq. 5
D_{53},etc.	= special cases of the generalized mean diameter
$\langle K_i \rangle$	= mean extinction coefficient for wavelength λ_i as defined by Eq. 12
l	= optical path length
m	= refractive index
n_0	= total number of particles in a given population or sample from a population.
$N[D_1 < D < D_2]$	= number of particles in the size range D_1 to D_2
$P[D_1 < D < D_2]$	= probability of occurrence of size greater than D_1 and less than D_2
t_{λ_i}	= spectral transmission for wavelength λ_i
δ	= shape constant in size distribution function
λ_i	= ith value of the wavelength of light
$\phi(D)$	= particle size distribution defined by Eq. (1)

Presented as Paper 69-146 at the AIAA 7th Aerospace Sciences Meeting, New York, January 20–22, 1969; submitted March 17, 1969; revision received March 30, 1970. This paper presents the results of one phase of research carried out at the Jet Propulsion Laboratory, California Institute of Technology, under Contract NAS 7-100, sponsored by NASA. The authors are indebted to A. Rasmussen and C. Feldstein for assistance with the rocket firings and the instrumentation, respectively. Computer programs for data reduction and calculation of mean extinction coefficients were written by M. R. Diethelm.

* Professor of Engineering. Member AIAA.
† Senior Engineer. Associate AIAA.

I. Introduction

THE importance of the particle size of aluminum oxide (Al_2O_3) produced in solid-propellant rocket motors has been appreciated from the time that metallic aluminum was first used as a fuel additive. A knowledge of particle size is required in order to calculate the thrust as influenced by two phase flow losses, particulate radiant heat transfer, particulate acoustic damping in the motor cavity, impingement of particles on nozzle entrance surfaces, and the rocket plume structure and its properties. Attempts to measure the particle size have resulted in a series of reports that describe observations differing sharply from one another and presenting contradictory conclusions. The disagreement seems to result from the normal difficulty of measuring populations of particles of widely varying sizes, compounded by the extreme environmental factors present in rocket motor chamber and nozzle. This work is concerned with a comparison of the results of two techniques of measuring particle size with which the authors possess first-hand experience. Our aim in this work has been to gain an understanding of the marked discrepancy that was reported between the results of these two techniques. We believe the present study has implications that impinge directly upon studies conducted by others, and we will comment on these implications at the conclusion of this report.

The background for the present work is provided by Fig. 6 of Ref. 1 where spectrophotometric tests indicate an increase in particle size by a factor of about 1.3, while the tank tests on essentially the same motor (described in Ref. 2) show a ten-fold increase in particle size when the chamber operating pressure increases from 70 to 700 psig. The hypothesis that the growth of size with pressure indicated by the tank tests might be caused by agglomeration of the particles in the recovery tank was advanced to explain this discrepancy.

Others later argued that agglomeration would occur in the rocket nozzle, and the photometric tests were unexplainable since they failed to indicate this growth. It was our belief at the outset of this study that the occurrence of particle growth in the nozzle because of the varying slip velocities would indicate that the tank collection technique could prove unsatisfactory, because of the shock waves and turbulent mixing that would occur within the tank at high recovery temperatures. Both shock waves and turbulence could cause further growth that might mask particle growth occurring within the nozzle. For these reasons, we planned a series of tank collection tests in which tank volume was a variable. A series of optical tests were also performed in which spectrophotometric measurements were made at three wavelengths of light rather than merely with two wavelengths as during the previous tests.

We consider the two methods of size measurement to be potentially complementary to one another because of their distinctive capabilities; the tank collection method gives a measure of the detailed size distribution averaged over the entire duration of firing, after a data reduction process that is tedious and time consuming; the optical technique measures a well-defined mean diameter of a large number of particles leaving the rocket nozzle on a time-resolved basis throughout the entire duration of the firing, and involves a data reduction process that requires only seconds to perform. The difficult feature of the tank test is the sampling and analysis of the collected sample. A drawback to the optical test is its failure to yield any information about the size distribution function and the small number of large particles that are present. A major goal of our effort has been to seek to realize the potential of using both methods in a mutually complementary manner.

Limitations of space prevent a description of much essential material on experimental procedures and certain other details. A technical report[3] on the present study is available in which the interested reader will find the important supplemental material.

II. Particle Size Statistics

A complete description of the "size" of polydispersed particles is provided if the particle size distribution function is known. The size distribution function $\phi(D)$, is defined such that

$$\int_{D_2}^{D_1} \phi(D)dD \equiv P(D_1 < D < D_2) \tag{1}$$

It is apparent that when D_1 is zero and D_2 corresponds to the largest size present, D_∞, then

$$\int_0^{D\infty} \phi(D)dD = 1 \tag{2}$$

the actual number of particles in the size range D_1 to D_2 will be

$$N(D_1 < D < D_2) = n_0 \int_{D_1}^{D_2} \phi(D)dD \tag{3}$$

Therefore,

$$\phi(D) = (1/n_0)dN(D)/dD \approx (1/n_0)\Delta N(D)/\Delta D \tag{4}$$

Equation (4) in incremental form provides a convenient expression to evaluate the size distribution function when size frequency data are presented as a bar histogram.

Under certain circumstances a full description of the particle size distribution function is unnecessary and only certain mean diameters or ratios of moments of the distribution function are required. The generalized mean diameter is commonly defined as

$$D_{PQ} \equiv \left[\int_0^{D\infty} \phi(D)D^P dD \Big/ \int_0^{D\infty} \phi(D)D^Q dD\right]^{1/(P-Q)} \tag{5}$$

The particular mean diameter, or ratio of moments, that is relevant is given by the detailed analysis of the partcular effect of interest. For example, Rannie[4] has analyzed the thrust loss because of the particle slip when the particle velocity and thermal lags are small. If we examine his analysis [in particular, Eqs. (72) and (80) of Ref. 4], we find that under certain circumstances, the ratio of the fifth moment to third moment of size distribution function,

$$D_{53} = \left[\int_0^{D\infty} \phi(D)D^5 dD \Big/ \int_0^{D\infty} \phi(D)D^3 dD\right]^{1/2} \tag{6}$$

can be used in the theory in the form appropriate for monodispersed particles. In other words, the D_{53} is the appropriate mean diameter to use in the theory for uniformly sized particles, i.e., a monodispersion, to correctly allow for the influence of the size distribution effects.

Table 1 Mean diameters relevant to various physical effects in gas-particle fluid mechanics and rocket technology

	Small size limit	Estimated usual case	Large size limit
Thrust loss due to particle slip[4]	D_{53}	D_{53}	...
Optical scattering power, optical measurement of particle size[5]	D_{63}	...	D_{32}
Acoustic damping[6]	D_{53}	D_{53}	D_{31}
Agglomeration due to particle lag[7]	D_{30}	D_{30}	...

In Table 1, we display the various mean diameters or moment ratios that are pertinent to various gas-particle flow phenomena. In most such phenomena, the relevant mean diameter will depend on how the particle sizes relate to a particular parameter. For example, if all particles in a distribution are small compared to the wavelength of light, the scattering power is related to the D_{63}. If all sizes in the distribution are large compared to λ, then D_{32} is the most relevant mean diameter. In the middle column of Table 1 we give, where possible, our estimate of the mean diameter that is relevant to rocket technology. In this study, the two mean diameters that assume special importance are the D_{32}, because this size is measured by the optical technique, and the D_{30}, because this moment ratio enters into the theory describing agglomeration due to slip.

Another method of characterizing mean particle size involves the use of the median diameter defined as

$$\int_0^{D_m} \phi(D)D^i dD = \frac{1}{2}\int_0^{D\infty} \phi(D)D^i dD \tag{7}$$

We will use the volume median diameter, for which $i = 3$, in order that our results may be related to other investigations. The median diameter has no theoretical usefulness except insofar as it may correlate with a relevant mean diameter.

Many different algebraic functions have been used to describe particle size distributions. We will be concerned with the log-probability function

$$\phi(D) = \{C_1 \exp - [\delta \ln_e(D/D_m)]^2\}/D^4 \tag{8}$$

and the upper limit function proposed by Mugele and Evans[8]

$$\phi(D) = \{C_2 \exp - [\delta \ln_e aD/(D_\infty - D)]^2\}/D^4(D_\infty - D) \tag{9}$$

The constants a and δ control the shape of the size distribution functions represented by Eqs. (8) and (9). Since Eq. (8) has a single shape constant and Eq. (9) has two, the latter expression has greater flexibility and generality. The constants C_1 and C_2 in Eqs. (8) and (9) are chosen so as to normalize the integrals to unity per Eq. (2). From Eq. (5), we see that it is unnecessary to evaluate the constants in calculating the mean diameters.

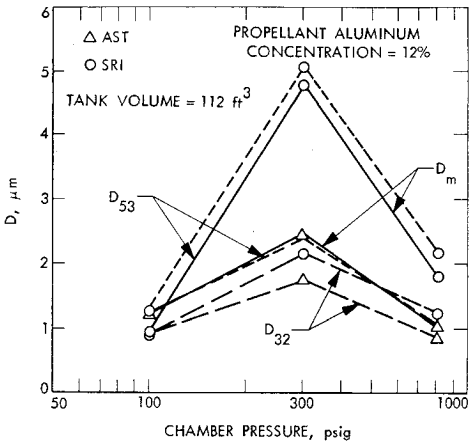

Fig. 1 Comparison of D_{53}, D_{32}, and D_m measured by two subcontractors.

A wide variety of other distribution functions have been proposed, and most all of them including Eq. (8) suffer from the drawback that they fail to provide for a finite value for D_∞. The consequences of this failure were examined in detail by Mugele and Evans[8] who have demonstrated the considerable merit to the function they have proposed.

III. Tank Collection Tests

Thirty small-motor firings were conducted in one series, using a tank collection technique, to determine whether the particle size distribution of the particulate effluent was dependent upon the size of the receiver tank. The test firings were conducted in five different recovery tank size configurations, covering a tank volume interval of from 40 to 168 ft³. The test program consisted of two test firings carried out at each of three motor chamber average pressures (100, 300, and 800 psi) for each of the five tank configurations. The motor chamber pressures were adjusted by varying the nozzle throat diameter (0.970, 0.705, and 0.480 in., respectively). For each test, the particulate effluent deposited in the tank was collected for particle size analysis. The details of the test and data reduction procedures are given in Ref. 3.

Electron microscope size analyses of a majority of the test samples were performed,‡ using essentially the same procedure as reported in Ref. 2. The raw photomicrographic data were processed by means of a computer program which calculated the distribution function of the parent population, the various mean diameters D_{54}, D_{43}, D_{32}, D_{21}, D_{10}, D_{53}, and D_{30} and also the volume median diameter D_m. The total mass of the 2000–4000 particles counted was calculated and expressed as a fraction of the total amount of aluminum oxide produced by the motor. The small magnitude of this quantity, typically 10^{-12}–10^{-14}, emphasizes the critical nature of the sampling procedure and the desirability of duplication of tests.

The computer program also generated quantities $\psi_1 = \ln(10D/D_\infty)$ and $\psi_2 = \ln[10D/(D_\infty - D)]$ as a function of the volume fraction of the parent population. The appropriateness of the log probability and the upper limit distribution functions, respectively, are revealed by plotting ψ_1 and ψ_2 against volume fraction on probability graph paper. The data usually resulted in a weakly S shaped curve on the log probability presentation. The upper limit presentation was roughly a straight line except at the smallest sizes, where the slope of the line decreased. Many experimentally measured distribution functions deviated from these general descriptions. The upper limit distribution function was considered more satisfactory because the data points more nearly formed a straight line with this presentation. This trend supports the more detailed discussion by Mugele and Evans[8] on the advantages of the upper limit function which they originated.

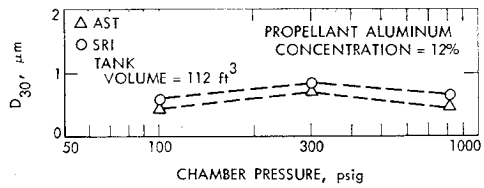

Fig. 2 Comparison of D_{30} measured by two subcontractors.

‡ Applied Space Technology Inc., Palo Alto, Calif.

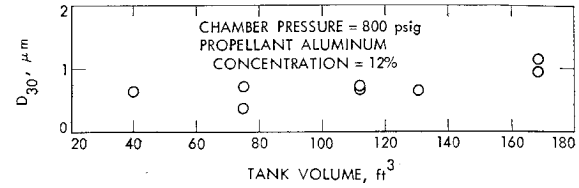

Fig. 3 Variation of D_{30} with recovery tank volume.

Additional electron microscopic analyses were performed on five of the test samples by the commercial laboratory§ that did the analysis work for Ref. 2 in order to test the statistical validity of the sampling and photo-micrographic procedures. The data reduction of these analyses shows that the high moments of the size distribution function show wide scatter when the results of one subcontractor's tests were compared with another. This is illustrated in Fig. 1, where D_{53}, D_{32}, and D_m, in micrometers (μm), are plotted against chamber pressure. The high scatter is caused by the occurrence of a small number of large particles that are difficult to sample properly and that totally dominate the size analysis. Thus, an accurate measurement of the high moments of the distribution function or the volume median diameter D_m is very difficult to obtain. Lower moments of the distribution function such as D_{30}, D_{21}, and D_{10} show reduced scatter because they are less sensitive to the occurrence of one or two large particles.

In view of the generalized definition of the mean diameter D_{PQ} [Eq. (5)], we find

$$D_{30} = (D_{32}D_{21}D_{10})^{1/3} \tag{10}$$

Thus, the D_{30} is a geometric average over one high moment and two low moments of the size distribution function. For this reason, and also because of the importance of this moment ratio in particle agglomeration theory, we will report primarily the D_{30} and will relate other moments to the D_{30}. A graph of the D_{30} vs chamber pressure for the same size analyses is shown in Fig. 2 and shows a substantial reduction in the scatter between the results by the two subcontractors. The D_{21} usually showed low scatter comparable to the D_{30}. The D_{10} tended to show greater scatter, apparently because of its sensitivity to the exact number of very fine particles that were counted.

The results of the series of tests conducted to determine if tank volume has an influence on the particle size is shown in Fig. 3, where D_{30} is plotted against tank volume at a constant pressure. No positive influence of tank volume on the D_{30} mean diameter is observed. The results of analysis of the data from tests in which tank size and pressure were systematically varied are depicted in Fig. 4, where D_{30} is plotted for three different tank sizes¶ at three rocket chamber

§ Sloan Research Industries Inc., Santa Barbara, Calif.

¶ Data obtained from the two smallest tank configurations were not used because, in some instances, these earliest samples were incorrectly handled.

Table 2 Description of spectrophotometer channels

Channel no.	Wavelength, μm	Bandpass, μm	Transducer
1	0.365	0.005	Type 1P21 photomultiplier
2	1.01	0.020	Type 7102 photomultiplier
3	2.35	0.040	Type N-2 lead sulphide cell

pressures. These tests show no systematic dependence of particle size on tank volume and show a weak dependence on chamber pressure.

The results of additional tests performed in the 168 ft^3 tank are shown in Fig. 5. In the tests in which aluminum fraction was varied from 2% (three tests) to 20% (one test), shown along with the corresponding results with 12% aluminum, the scatter in the data is moderate, but no systematic variations of particle size with the aluminum loading in the propellant is noted. In the second series of additional tests, the motor nozzle was removed and the motor pressure was controlled by prepressurizing the tank motor assembly with nitrogen. The results of these two single firings are also plotted on Fig. 5. They show high scatter and are considered inconclusive.

We conclude from the tank tests that particle size is not sensitive to the volume of the collection tank, is not influenced by the aluminum loading in the propellant, and is weakly influenced by chamber pressure.

A limited chemical and physical analysis was made of the material recovered from the tank, which was a grey-green powder. Electron diffraction measurements were performed which indicated that the smallest particles were mainly γ-Al_2O_3 and the largest particles were principally α-Al_2O_3. These observations are in agreement with measurements of refractive index (see below). The recovered material was analyzed for carbon by oxidation and gas chromatography. The average carbon content for several samples, each from the effluent recovered from the rocket motor with varying propellant fraction of aluminum was as follows: 20% Al, 0.11% C; 12% Al, 0.18% C; 2% Al, 0.57% C. The discoloration of the material from the white appearance displayed by pure powdered Al_2O_3 suggests that impurities originating in the combustion process were present. Examination of the material by optical microscopy indicated that many particles possess an orange cast and that a few of the particles contained an opaque core—possibly composed of metallic aluminum. These observations suggest to us that the imaginary portion of the refractive index for the particulate effluent from rocket motors may be substantially different from the low values applicable to pure Al_2O_3.

IV. Spectrophotometric Tests

During the present investigation, we have performed additional spectrophotometric tests using the emission-scattering photometer. The theory and operation of this device have been described in Ref. 1 and the references therein. This photometer was modified by the inclusion of an additional monochromator in place of the unit previously noted as a filter and IR detector (Fig. 2 of Ref. 1). The signal from this detector was amplified and recorded in the same manner as the other two signals. Table 2 summarizes the information on wavelengths and bandpass width for the three channels of the spectrophotometer.

The refractive index of the particulate effluent of the rocket motor is required in order to allow an interpretation of the spectrophotometric tests. For this reason the refractive index of the effluent material was measured by the immersion method[9] using a 400 X optical microscope. The refractive index at $\lambda = 0.59$ μm varied systematically over the range from 1.744 to 1.665 as particle size decreased. This result is in agreement with the observations by electron diffraction

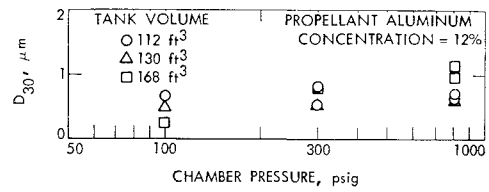

Fig. 4 Variation of D_{30} with chamber pressure and collection tank volume.

patterns that indicate a large fraction of γ-Al_2O_3 as particle size decreases. We consider that a mean value of $m = 1.71$ at $\lambda = 0.59$ μm for the cold particulate effluent is a reasonable value. We estimate the refractive index at the various wavelengths as follows. The refractive index of pure sapphire[10] at $\lambda = 0.59$ μm is 1.76, or 0.05 greater than that of the particulate effluent. We arbitrarily apply the -0.05 correction to the refractive index of pure sapphire. Gryvnak and Burch[11] have estimated, from experimental observations, the change in refractive index of sapphire to be $+0.05$ when temperature is increased from 25° to 1700°C. This temperature is reasonably representative of the temperature of the particles at the rocket nozzle exit plane where the observations of size are made. Thus, our estimate is that values for the real part of the refractive index of sapphire are, fortuitously, the values applicable to the particulate effluent at the nozzle exit plane and in the near plume.

The estimates of absorption coefficient of pure aluminum oxide given by Gryvnak and Burch indicate that the imaginary portion of the refractive index is on the order of 10^{-6}. However, our expectation is that the refractive index of the particulate effluent is dominated by the impurity content that is responsible for its strong coloration. Calculations of $\langle K_i \rangle$ for values of the imaginary portion of refractive index as large as 10^{-2} are cited in Ref. 3, and they indicate that spectral opacity is not significantly affected.

The data on optical transmission of the rocket plume are analyzed by the following procedure. The spectral transmission for polydispersed particles can be expressed[1] as

$$\ln t_{\lambda_i}^{-1} = \tfrac{3}{2}\langle K_i \rangle c_v l / D_{32} \tag{11}$$

and the mean extinction coefficient, $\langle K_i \rangle$ is given by

$$\langle K_i \rangle = \int_0^{D\infty} K\left(\frac{\pi D}{\lambda_i}, m\right) \phi(D) D^2 dD \Big/ \int_0^{D_\infty} \phi(D) D^2 dD \tag{12}$$

where m is the (complex) refractive index and is in general a function of λ_i, the wavelength of light. The values of $\langle K_i \rangle$ are calculated using the upper limit size distribution function given by Eq. (9). If we divide the transmission equations for two different wavelengths, λ_i and λ_j, by one another we find

$$\langle K_i \rangle / \langle K_j \rangle = \ln t_i^{-1} / \ln t_j^{-1} \tag{13}$$

From calculations of mean extinction coefficients, we find the ratio $\langle K_i \rangle / \langle K_j \rangle$ is, under certain circumstances, uniquely related to D_{32} for given λ_i and λ_j and corresponding values of m. Thus, optical transmission conducted simultaneously at

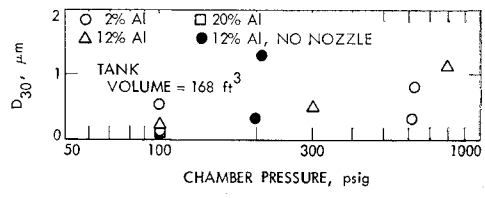

Fig. 5 Variation of D_{30} with aluminum loading and chamber pressure.

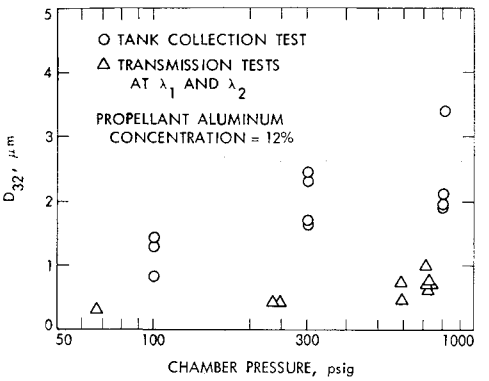

Fig. 6 Comparison of D_{32} measured by tank collection and optical transmission tests.

two suitable chosen wavelengths of light can be related to the D_{32}.

The purpose of adding the third channel to the spectrophotometer was to determine if the various combinations of transmission data indicated a consistent particle size. The optical tests were conducted with the same propellant composition, configuration, and rocket motor as was used in the tank firings. Good data were obtained in all but two of the 28 test firings. The tests included a repetition of some of the previous tests[1] and also a series in which the aluminum loading in the propellant was varied. Further details are discussed in Ref. 3.

Data reduction of the firings of propellants with 12% aluminum in the propellant indicated the following points: 1) when the mean extinction coefficients [Eq. (12)] were calculated with the shape parameters for the upper limit distribution function [Eq. (9)] equal to the values used previously,[1] namely $a = 1.13$ and $\delta = 1.26$, the value of D_{32} indicated by tests at λ_2 and λ_3 was about 2–2.5 times greater than the size indicated by tests at λ_1 and λ_2, and 2) the D_{32} indicated by tests at λ_1 and λ_2 was about one-third the value of D_{32} indicated by the tank collection tests.

This comparison is shown in Fig. 6. (The reduction of the spectrophotometric data presented in Fig. 6 was accomplished with shape parameters of $a = 1.0$ and $\delta^2 = 0.50$. This data reduction gives virtually the same result for the case when $a = 1.13$ and $\delta = 1.26$ because the mean size is weakly dependent upon the shape of the size distribution function. This is the basic principle upon which the spectrophotometric method rests, and it is discussed in detail in Ref. 12.)

These discrepancies were believed to be caused by a radical departure of the distribution function from its assumed form. For the shape parameters $a = 1.13$, $\delta = 1.26$, the distribution function is a skewed monomodal curve, depicted in Fig. 3 of Ref. 12. The size distributions obtained from reduction of tank collection data showed substantially more skewness and often decreased monotonically from the smallest size increment.

New values of the shape parameters were found by matching approximately the various ratios of mean diameters such as D_{21}/D_{30} and D_{21}/D_{10}. Ratios of low moments were preferred because these quantities were considered most accurately

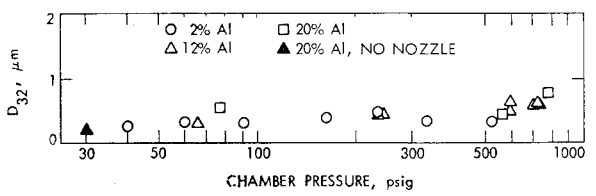

Fig. 7 Measurement of particle size (D_{32}) from transmission tests at λ_1 and λ_2.

measured by the tank collection tests. In the first column of Table 3, we show the values of six different mean or median diameter ratios as determined by averaging the values of these numbers over ten individual tests at three pressures and three collection tank sizes. We did not observe any systematic variation of these ratios with either chamber pressure or tank size. The same ratios can be calculated for the upper limit function using expressions given by Mugele and Evans[8] for the quantities D_{32}/D_∞, D_{31}/D_∞, D_{30}/D_∞; by noting that $D_m/D_\infty = 1/(1 + a)$ and by using Eq. 5 to develop a relation for D_{21}/D_∞. The ratio D_{53}/D_∞ was evaluated by a numerical integration procedure using Simpson's Rule. Values of $a = 0.85$ and $\delta = 0.62$ were found by trial and error to match D_{21}/D_{30} and D_{21}/D_{10} with good accuracy, although some other ratios do not match well, as is apparent by examining columns 1 and 2 of Table 3.

One interesting trend revealed by the data analysis was a good correlation between the median diameter D_m and the D_{53}. The ratio of $D_{53}/D_m = 1.11$ for the average of the ten data points. Thus, we find that the shape of the distribution function is, fortuitously, such that the D_m and D_{53} nearly coincide. The D_m, which has been used in past studies of the size of Al_2O_3 from rocket motors, is an appropriate diameter to use to calculate thrust penalty due to gas particle flow losses. This conclusion rests on the fulfillment of the various assumptions of Rannie's theory[4] for the calculation of two-phase thrust penalty.

Mean extinction coefficients were calculated for the upper limit function with other combinations of shape parameters a and δ. The mean size D_{32} yielded by both combinations of a and δ listed in Table 3 gives essentially the same results. The use of either of these combinations of shape parameters failed to eliminate a factor of about 2 in the discrepancy between the sizes indicated by the wavelength combinations $\lambda_1 - \lambda_2$ and $\lambda_2 - \lambda_3$, respectively. Throughout this work the data reduction was accomplished using the shape parameters $a = 1.0$, $\delta^2 = 0.50$. Values of $\langle K_i \rangle$ for the λ_i values for this combination of parameters are given in Ref. 3 for various values of D_{32}.

A study of possible reasons for the discrepancy between the sizes predicted by the two different combinations of wavelengths is given in Ref. 3. The results may be summarized as follows: Since no continuous monomodal distribution was found that rendered a consistent indication of size, it is concluded that the true size distribution is bimodal.

The transmission tests at wavelengths λ_1 and λ_2 are found to be of a proper selection to allow the small-size distribution to be measured. The transmission test at λ_3 is sensitive to the large sizes, which in small samples appear as discrete spectra, but would require a transmission test at a fourth suitably selected wavelength in order to permit quantitative interpretation in terms of the mean size of the large size spectrum. The transmission test data at λ_3 are not useful except as a nonquantitative, positive indication of the bimodal character of the size distribution function.

Table 3 Values of various ratios of mean diameters

Ratio	Experimental[a] values	Upper limit functions $a = 0.85$, $\delta = 0.62$	Upper limit function $a = 1$, $\delta^2 = 0.5$
D_{53}/D_{30}	5.17	3.47	3.81
D_m/D_{30}	4.66	3.40	2.454
D_{21}/D_{30}	1.13	1.18	1.11
D_m/D_{32}	1.55	1.42	1.32
D_{21}/D_{10}	3.13	3.34	2.29
D_{32}/D_{30}	3.00	2.39	1.85

[a] Average values for ten tests at three different pressures and three tank sizes: ratios were not observed to vary systematically with tank size or pressure.

A number of optical tests were conducted with the aluminum loading in the propellant varied. We interpret this series of tests within the context of the above model. The results are shown in Fig. 7, where we find particle size is weakly influenced by aluminum loading. This is in agreement with results of the tank collection tests (Fig. 5).

V. Comparison of Experimental Results with Theory for Particle Agglomeration due to Slip and Collision

The experimental results can be interpreted using the theory for agglomeration of particles due to slip and collision by Marble.[7] The details of this calculation are given in Ref. 3, and we summarize the results here. For the experimental data given in Fig. 4, we find the increase in D_{30} for a motor pressure range of 100–800 psig to be by a factor of about 1.72 for a propellant aluminum concentration of 12% (22.7% Al_2O_3 in exhaust gases). If we attribute this increase in particle size to growth by particle slip and collision in the nozzle, then an experimental value of the agglomeration constant can be calculated. The experimental value of the agglomeration constant was found to be about 6.4% of the theoretical value.

A possible explanation for the large difference between the theoretical and experimental growth factors may be due to the high drag coefficients found in gas-particle flows.[13,14] High particle drag reduces slip velocities and agglomeration rates. An alternative explanation for the small observed agglomeration factor is the possibility that coalescence of the particles on contact may not occur.

The slight increase of particle size with motor pressure and the lack of dependency of particle size on propellant aluminum concentration (Fig. 7) are evidence that the slip and collision agglomeration mechanism of particle growth within the rocket nozzle is absent. Our results thus suggest that the mild particle growth with increased pressure results from mechanisms that influence the size of the particles before they reach the nozzle entrance.

In the previous discussion, we are comparing the low-moment ratios with a linearized theory that requires that the particles be such that slip velocities are small compared to gas velocity. It is possible that significant growth because of the particle lag can occur in sizes that are too large to be described by the linearized theory. We therefore examined the D_{53}, which is very nearly equal to the D_m, to see if evidence of more extreme growth was present in the high-moment ratios (Fig. 8). Here we found a growth factor of about 1.6 over an eight-fold pressure ratio. No systematic variation of D_{53} with aluminum loading was noted. The scatter of the data is very great, however, and we draw no conclusions on

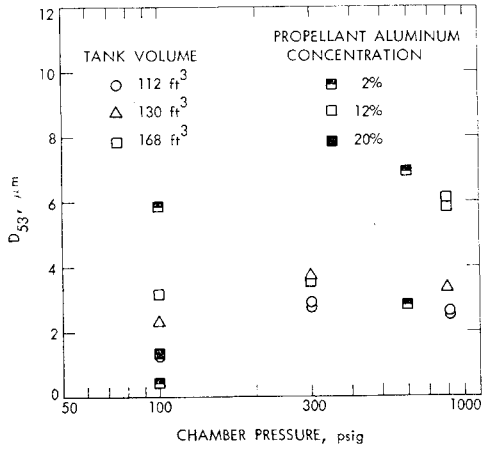

Fig. 8 Variation of D_{53} with collection tank volume, aluminum loading, and motor chamber pressure.

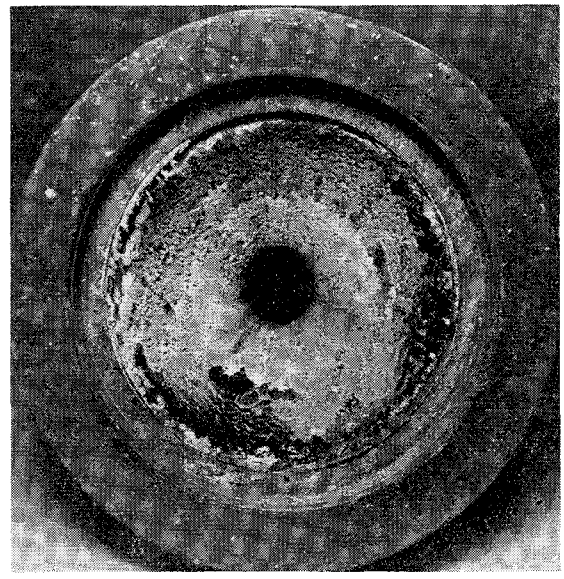

Fig. 9 Photograph of nozzle entrance surface showing erosion of the deposited layer of aluminum oxide.

the presence or absence of growth in the high-moment ratios from our tests. The scatter is attributed to the extreme difficulty in sampling the large-size tail of the size-distribution function.

VI. Comparison with Results of Other Investigators

The results of this study can be compared with other tank collection studies by Crowe and Willoughby.[15] They conducted an extensive series of firings into a tank using rocket motors and propellants comparable to those used in this program. One difference in the test procedures should be noted. In this program, motor chamber pressure was controlled by varying nozzle throat area; in the study by Crowe and Willoughby the nozzle throat area was fixed and the propellant surface area was varied.

Their experimental results, reported as mass median particle sizes, indicate a marked growth of particle size with rocket chamber pressure and a lesser amount of growth when the same rocket motors were fired, with nozzle removed, into a prepressurized tank. These results were interpreted to indicate that particle growth because of the collision and agglomeration occurred in the rocket nozzle. This conclusion is in conflict with the conclusions of this investigation. Another possible explanation is that the presence of the rocket nozzle provides a surface for the deposition of a liquid layer of Al_2O_3 which is subsequently shed to form large particles by the viscous shear forces of the boundary layer. Figure 9 is a photograph of the interior surface of a rocket motor end closure. Small crevices formed by aerodynamic erosion of this layer are apparent. At high aluminum loadings and small nozzle throat diameters the thickness of this layer was sufficient to cause loss of control of chamber pressure.

We advance the hypothesis that the particle size observed by Crowe and Willoughby in their tests on motors equipped with nozzles increased because the nozzle served as a surface on which deposition and erosion occurred and that the erosion of this deposited layer was the source of the large particles. This hypothesis provides an explanation for many of the results of the present study and that of Crowe and Willoughby.

VII. Summary and Conclusions

Tank collection tests of Al_2O_3 particles produced by a small rocket motor indicate that particle size is 1) independent of

receiver tank capacity, 2) independent of aluminum concentration within the propellant, and 3) weakly dependent on rocket motor chamber pressure, i.e., size increases by a factor 1.7 with a ten-fold increase in pressure.

Spectrophotometric tests were conducted using transmission measurements at three wavelengths of light. The tests yielded internally inconsistent results in that the magnitude of mean size D_{32} differed by a factor of about 2 depending on which combination of wavelengths were used. (To explain this discrepancy, it is necessary to postulate a bimodal size distribution function.) The influence of aluminum loading and chamber pressure on the size of the particulate effluent was found to be identical in both tank collection and spectrophotometric tests.

Based on the previous results, we conclude that the low-moment ratios of the Al_2O_3 particles show no evidence of growth by velocity slip and collision during their passage through the rocket nozzle. Such a mechanism would be sensitive to both changes in chamber pressure and aluminum loading. We draw no conclusions on the possibility of growth of the high-moment ratios because the data on these ratios display very high scatter. The scatter is attributed to the extreme difficulty in sampling the large-size tail of the particle-size distribution function.

The only point of disagreement between this study and the results of Crowe and Willoughby is the mechanism for the production of the large particles. Evidence is presented indicating that this mechanism is the aerodynamic shedding of Al_2O_3 deposited on the nozzle entrance and lateral surfaces.

The impurities present in the primarily Al_2O_3 particulate effluent from the rocket motor control the coloration of the material. These impurities probably exert a dominate effect on the imaginary portion of the refractive index at high temperatures. The use of the imaginary portion of the refractive index measured for pure Al_2O_3 as representative of rocket motor particulate effluent in particulate radiant heat-transfer calculations appears unjustifiable to the authors.

References

[1] Dobbins, R. A., "Remote Size Measurements of Particulate Products of Heterogeneous Combustion," *Eleventh Symposium (International) on Combustion*, The Combustion Institute, 1967, p. 921.

[2] Sehgal, R., "An Experimental Investigation of a Gas-Particle Flow System," TR 32-238, March 1962, Jet Propulsion Lab., Pasadena, Calif.

[3] Dobbins, R. A. and Strand, L. D., "A Comparison of Two Methods of Measuring Particle Size of Al_2O_3 Produced by a Small Rocket Motor," TR 32-1383, June 1969, Jet Propulsion Lab., Pasadena, Calif.

[4] Rannie, W. D., "Perturbation Analysis of One-Dimensional Heterogeneous Flow in Rocket Nozzles," *Progress in Astronautics and Rocketry*, Vol. 6, Academic Press, New York, 1962, p. 117.

[5] Dobbins, R. A., "Measurement of Mean Particle Size in a Gas-Particle Flow," *AIAA Journal*, Vol. 1, No. 8, Aug. 1963, p. 1940.

[6] Dobbins, R. A. and Temkin, S. "Attenuation and Dispersion of Sound by Particulate Relaxation Processes," *The Journal of the Acoustical Society of America*, Vol. 40, 1966, p. 317.

[7] Marble, F. E., "Droplet Agglomeration in Rocket Nozzles Caused by Particle Slip and Collision," *Astronautical Acta*, Vol. 13, 1967, p. 159.

[8] Mugele, R. A. and Evans, H. D. "Droplet Size Distribution in Sprays," *Industrial and Engineering Chemistry*, Vol. 42, 1951, p. 1317.

[9] Kerr, P. F., *Optical Mineralogy*, 3rd ed., McGraw-Hill, New York, 1959, p. 143.

[10] Malitson, I. H. et al, "Refractive Index of Synthetic Sapphire," *Journal of the Optical Society of America*, Vol. 48, 1958, p. 72.

[11] Gryvnak, D. A. and Burch, D. E., "Optical and Infrared Properties of Al_2O_3 at Elevated Temperature," *Journal of the Optical Society of America*, Vol. 55, 1965, p. 625.

[12] Dobbins, R. A. and Jizmagian, G. S., "Optical Scattering Cross Sections for Polydispersions of Dielectric Spheres," *Journal of the Optical Society of America* Vol. 56, 1966, p. 1345.

[13] Rudinger, G., "Effective Drag Coefficients for Gas Particle Flow in Shock Tubes," *Transactions of the ASME, Ser. D: Journal of Basic Engineering*, Vol. 92, 1970, p. 165.

[14] Selberg, B. P. and Nicholls, J. A., "Drag Coefficients of Small Spherical Particles," *AIAA Journal*, Vol. 6, No. 3, March 1968, p. 401.

[15] Crowe, C. T. and Willoughby, P. G., "A Study of Particle Growth in a Rocket Nozzle," *AIAA Journal*, Vol. 5, No. 7, July 1967, p. 1300.